Research Article

Shaysh Aziz Mohammed* and AbdulMuttailb I. Said

Analysis of concrete beams reinforced by GFRP bars with varying parameters

https://doi.org/10.1515/jmbm-2022-0068
received April 13, 2022; accepted May 01, 2022

Abstract: Structural buildings consist of concrete and steel, and these buildings have confronted many challenges from various aggressive environments against the materials manufactured from them. It contains high water levels and buildings whose concrete cover may be damaged and thus lead to the deterioration and corrosion of steel. It was important to have an alternative to steel, such as the glass fiber reinforced polymer (GFRP), which is distinguished by its great effectiveness in resisting corrosion, as well as its strong tensile resistance. Still, one of its drawbacks is that it has a low modulus of elasticity. This research article aims to conduct a numerical study using the nonlinear finite element ABAQUS program on eight beam models with various parameters such as stirrup spacing, compressive strength, reinforcement layer, and type of bar reinforcement under four-point bending. The result shows that the ultimate load capacity of the GFRP beam is higher than that of a beam reinforced with steel and the number and width of cracks are greater in the GFRP-reinforced beam than in the steel-reinforced beam. In general, the serviceability reflected by cracks and deflection is lower in GFRP-reinforced beams than in steel-reinforced beams with higher serviceability. The results, on either hand, showed the expected behavior of GFRP, which is linear elastic to the failure stage. These beams are divided into four groups of beams with different variables studied to understand GFRP bars' behavior under static loading. The variables taken in this study are the spacing between the stirrups, the compressive strength of concrete, the effect of the number of layers of reinforcement, and the type of reinforcement bar.

Keywords: GFRP bars, deflection, concrete, steel bar, cracks, ductility

1 Introduction

Steel and concrete are basic and commonly used materials in several buildings. Due to the plenty of use of these materials in construction, it was necessary to work on finding alternatives with better properties at all levels. Steel was one of these essential elements that were the focus of attention of engineers and researchers. The previous researchers explained that a fiber-reinforced polymer (FRP) was one of the appropriate materials to give better properties than steel in several aspects, including lightweight compared to steel, higher tensile strength than steel [1–4], and not affected by electric and magnetic fields which are advantageous for their use in civil infrastructure. Furthermore, since they are non-conductive, they are suitable for medical applications that are highly sensitive to electromagnetic fields, including magnetic resonance imaging facilities [5]. Also, most importantly, it does not cause corrosion or be affected by moisture, as is the case in steel or concrete buildings. According to the ACI 440 guide [6], over-reinforcing glass fiber reinforced polymer (GFRP)-reinforced concrete beams are required so that they fail due to concrete crushing rather than rebar rupture. The flexural behavior of GFRP of reinforced concrete beams exhibits negligible ductility due to the linear elastic brittle behavior of GFRP bars. A beam or structural member can sustain inelastic deformation without losing its ability to resist loads before failure is known as ductility [7]. The beams were chosen as one of the essential parts of the building whose behavior must be studied during the use GFRP bars as a substitute for steel and to know the extent to which they are affected by the direction of flexural behavior and stresses. Nonlinear finite element analysis will be carried out using the ABAQUS computer program to simulate the behavior of such beams under four-point bending.

* **Corresponding author: Shaysh Aziz Mohammed,** Civil Engineering Department, College of Engineering, University of Baghdad, Baghdad, Iraq, e-mail: Shaysh96@outlook.com
AbdulMuttailb I. Said: Civil Engineering Department, College of Engineering, University of Baghdad, Baghdad, Iraq, e-mail: dr.abdulmuttalib.i.said@coeng.uobaghdad.edu.iq

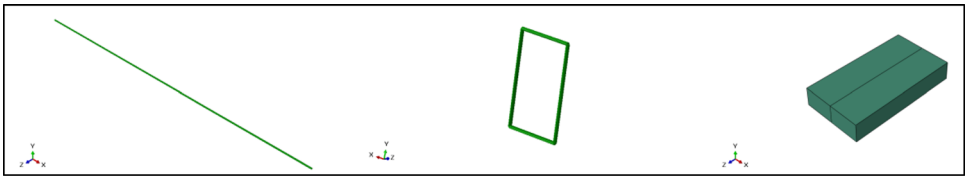

Figure 1: Parts of beam model.

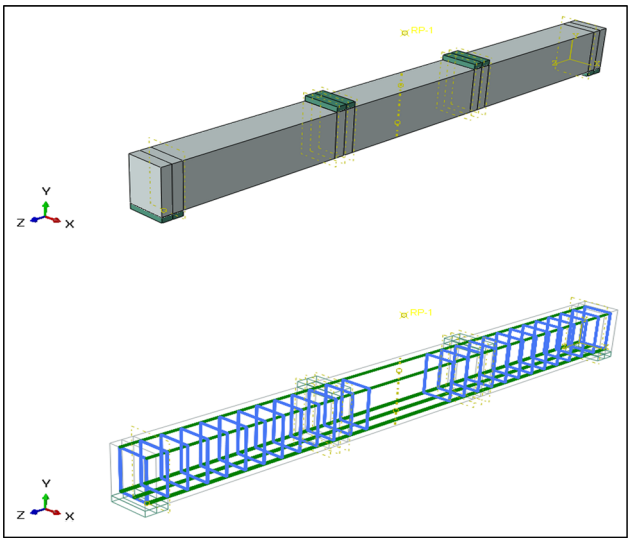

Figure 2: Assembly of beam.

1.1 Modeling of beams

The beams were modeled under four-point bending using the ABAQUS program and using different theories to understand the behavior of GFRP and introduce the program for it to reach convincing scientific results. The models of the materials utilized are determined by their qualities and theories adopted which are divided into two parts. The first part of the theory of concrete representation is the use of the common model, which is concrete damaged plasticity, which is close to the smeared cracking model, but is closer to reality. The second part is concerned with the representation of steel, where the classical metal plasticity theory was used [8]. This theory is based on a standard Mises model with associated plastic flow known as von Mises yield surface. The beam parts consist of GFRP and steel bars, stirrups, and bearing plates (Figure 1).

These parts are defined according to the materials manufactured in the property field, where the concrete properties of elastic behavior and plasticity parameters of concrete damage were defined [9]. After concrete, the properties of GFRP and steel are defined, which are elasticity and plasticity parameters, the Young's modulus and Poisson's ratio. Finally, bearing and support plates defined as steel materials with the properties of elastic steel. In the next stage of the modeling, the beam parts are assembled, then the nature of the loads applied to the beams are defined, which are static loads. Figure 2 shows the beam after assembly.

The interaction between all sections of the beams is described, and one of the most important parts is the nature of the relationship between concrete and GFRP, which is a perfect bonding relationship. Figure 3 shows the beam interaction. The next stage defines the loads and the boundary conditions represented by the hinge and roller. To obtain acceptable and good results, several attempts are made to reach the appropriate mesh size in the meshing stage. Figure 4 shows the beam meshing.

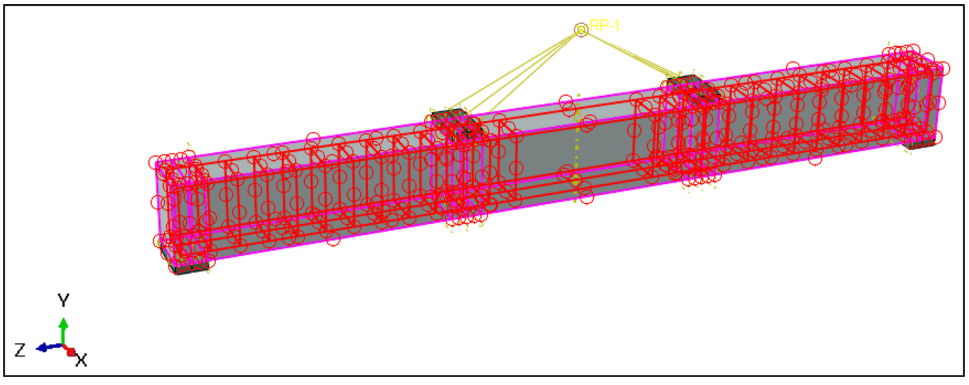

Figure 3: Interaction of beam.

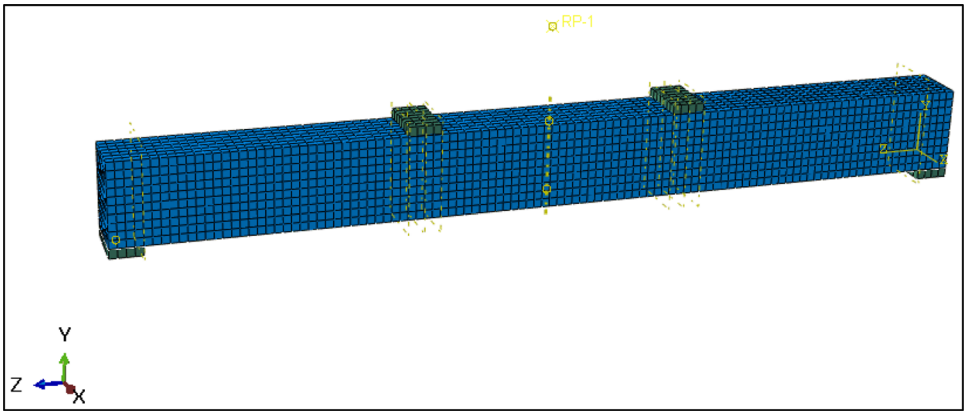

Figure 4: Meshing of beam.

Table 1: The specifics of modeling beams

Groups	Sample	Spacing (mm)	Compressive strength (MPa)	Bar top (mm)	Bar bottom (mm)
Group 1	A1	90	50	2 Ø 8	3 Ø 12
	A2	150	50	2 Ø 8	3 Ø 12
Group 2	B3	90	35	2 Ø 8	3 Ø 12
	B4	90	70	2 Ø 8	3 Ø 12
Group 3	C5	90	40	2 Ø 8	3 Ø 12
	C6	90	40	2 Ø 8	4 Ø 10
Group 4	GFRP	90	50	2 Ø 8	3 Ø 12
	Steel	90	50	2 Ø 8	3 Ø 12

1.2 Case study

In this study, a group of beams with different variables were studied to understand the behavior of GFRP bars under static loading. The variables taken in this study are the spacing between the stirrup, the compressive strength of concrete, the effect of the number of layers of reinforcement, and the type of reinforcement bar. The dimensions of the beams are the length of the beams is 2,700 mm, the clear span is 2,500 mm, the width of the beams is 180 mm, and the depth is 260 mm. These models are divided into four groups, each group consists of two beams, and the variables taken in this study are different for each group, the first group consists of two beams, and the spacing was changed between stirrup at different values of 90 and 150 mm. The second group consists of two beams and the compressive strength of the concrete was changed at different values of 35 and 70 MPa. In the third group, there are also two beams, and the reinforcement layers changed, once one layer (3 Ø 12 mm) and once two layers (4 Ø 10 mm). The fourth group consists

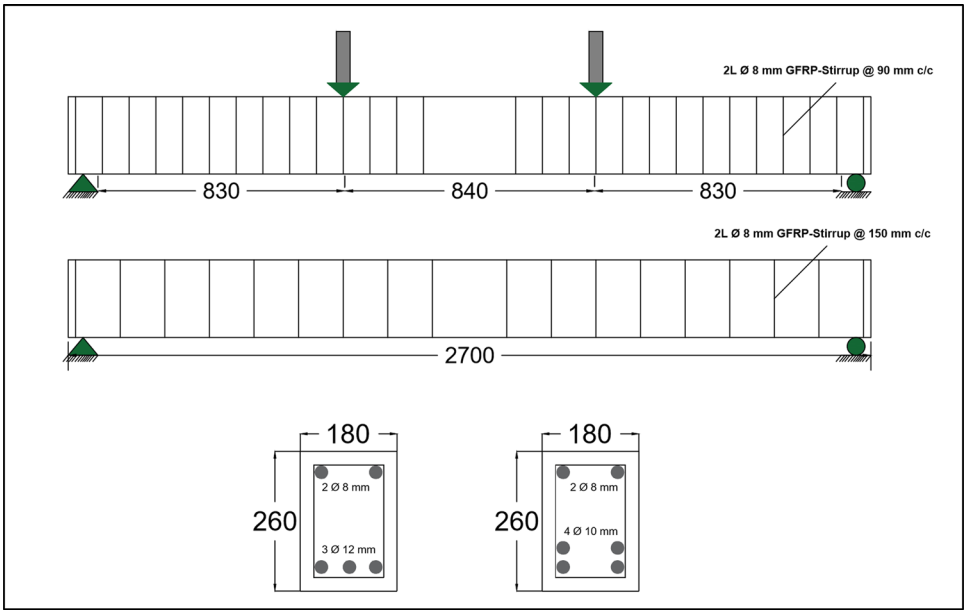

Figure 5: Beam details.

Table 2: The properties of bars

Type of bars	Tensile strength, f_y (MPa)	Rupture strain, ε	Modulus of elasticity, E (MPa)
GFRP	850	0.017	50,000
Steel	420	0.0021	200,000

Table 3: Damage of plasticity data

Parameter	ψ	ϵ	fb0/fc0	K	μ
Value	31	0.1	1.16	0.667	0.0001

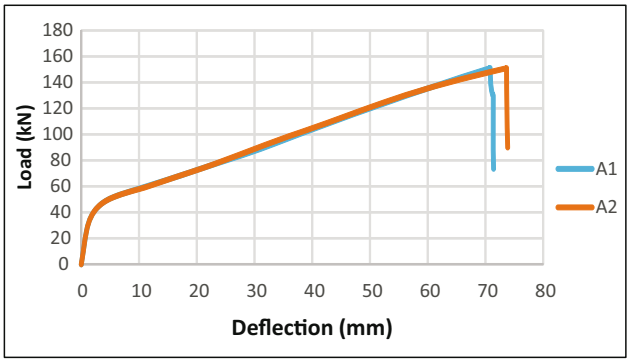

Figure 6: Load–deflection curve for specimens beams A1 and A2.

of two beams, the first beam is reinforced with GFRP bars and the second beam is reinforced with steel bars. Figure 4 and Table 1 show beam's details (Figure 5).

1.3 Properties of bars

GFRP bars are characterized by high tensile strength and low modulus of elasticity, which gives them a brittle behavior that leads to sudden failure, unlike steel, which has a high modulus of elasticity and has a higher ductility behavior. Table 2 shows the manufacturer's properties of GFRP and steel bars.

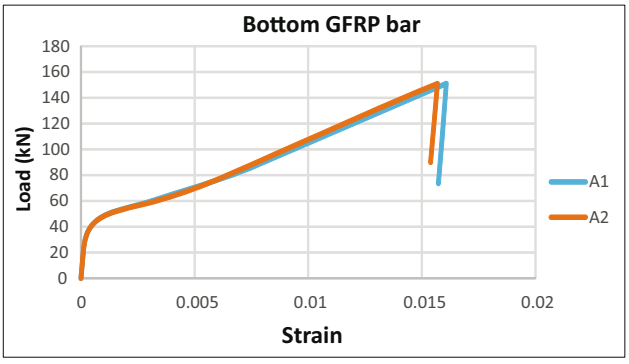

Figure 8: Strain of the bottom bar for specimens beams A1 and A2.

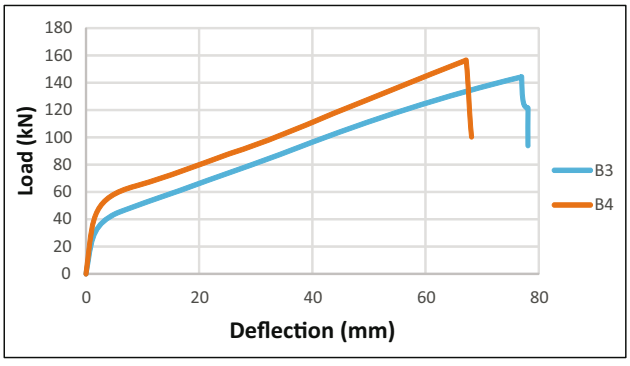

Figure 9: Load–deflection curve for specimens beams B3 and B4.

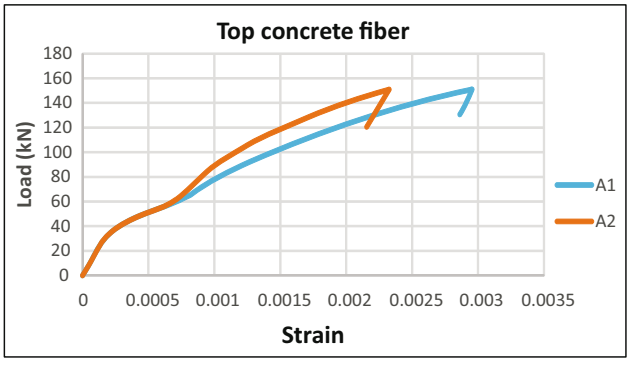

Figure 7: Strain in top concrete fiber for specimens beams A1 and A2.

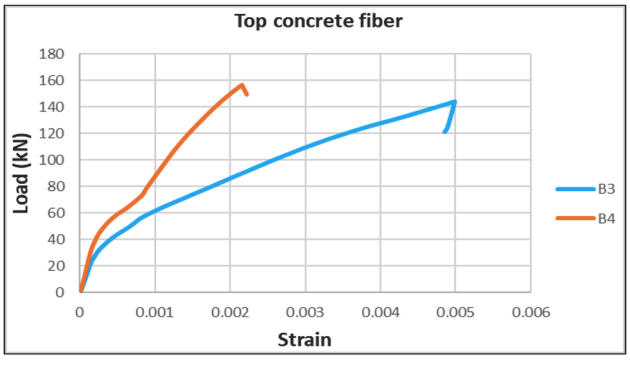

Figure 10: Strain in top concrete fiber for specimens beams B3 and B4.

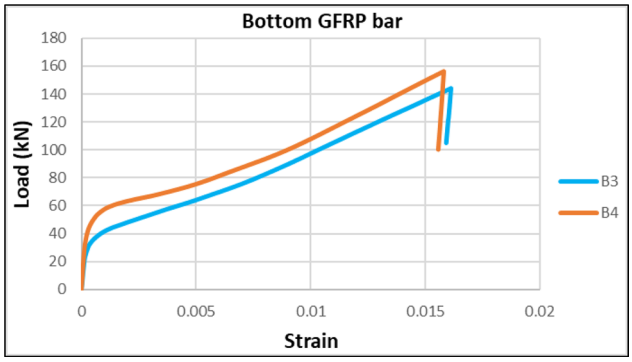

Figure 11: Strain of the bottom bar for specimens beams B3 and B4.

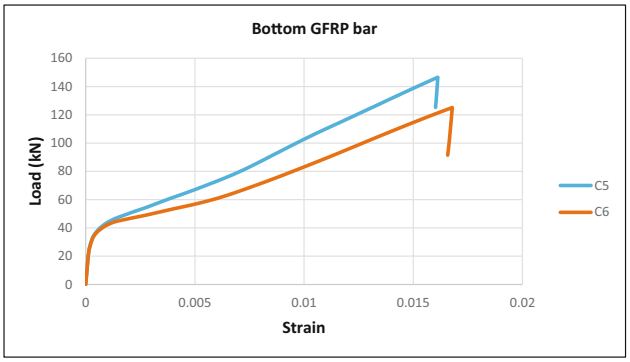

Figure 14: Strain of the bottom bar for specimens beams C5 and C6.

1.4 ABAQUS parameters

These parameters with these values came as a result of many previous research and studies in the field of the general behavior of concrete in its usual form in the theories of finite elements [10,11]. Table 3 shows the damage of plasticity data used in the models.

2 Results

After analyzing the beams using the ABAQUS 2019 software, and as expected, the results showed the behavior of the linear elastic GFRP rebar until the failure stage. In addition, there is no yielding point as in the case of steel rebar, and this is due to the characteristics of the FRP characterized as brittle, which leads to a sudden rupture

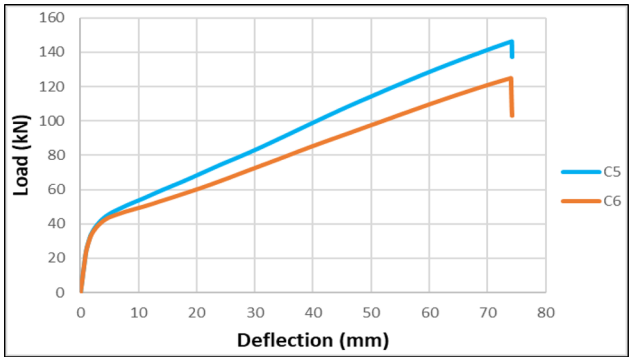

Figure 12: Load–deflection curve for specimens beams C5 and C6.

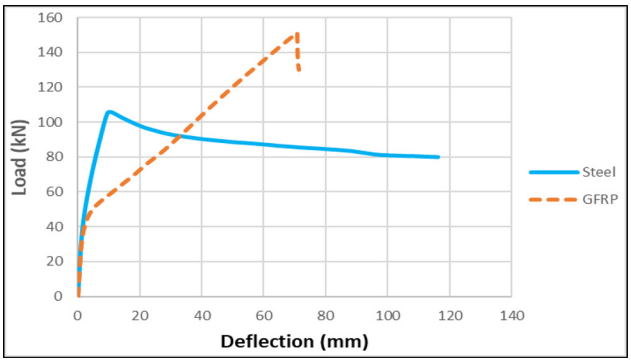

Figure 15: Load–deflection curve for specimens beams steel and GFRP.

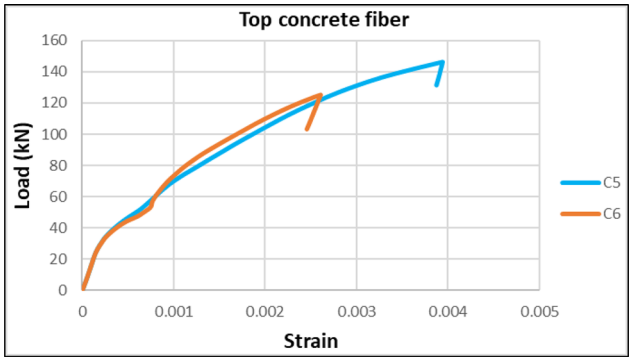

Figure 13: Strain in top concrete fiber for specimens beams C5 and C6.

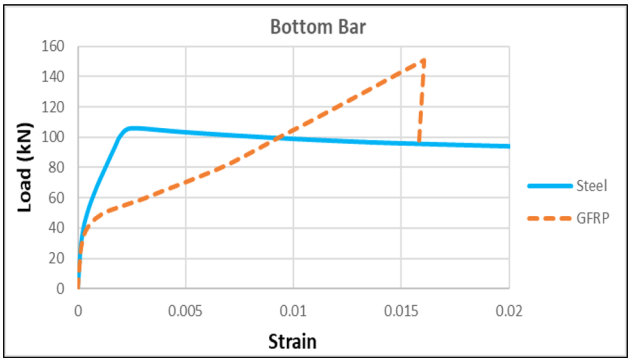

Figure 16: Strain of the bottom bar for specimens beams steel and GFRP.

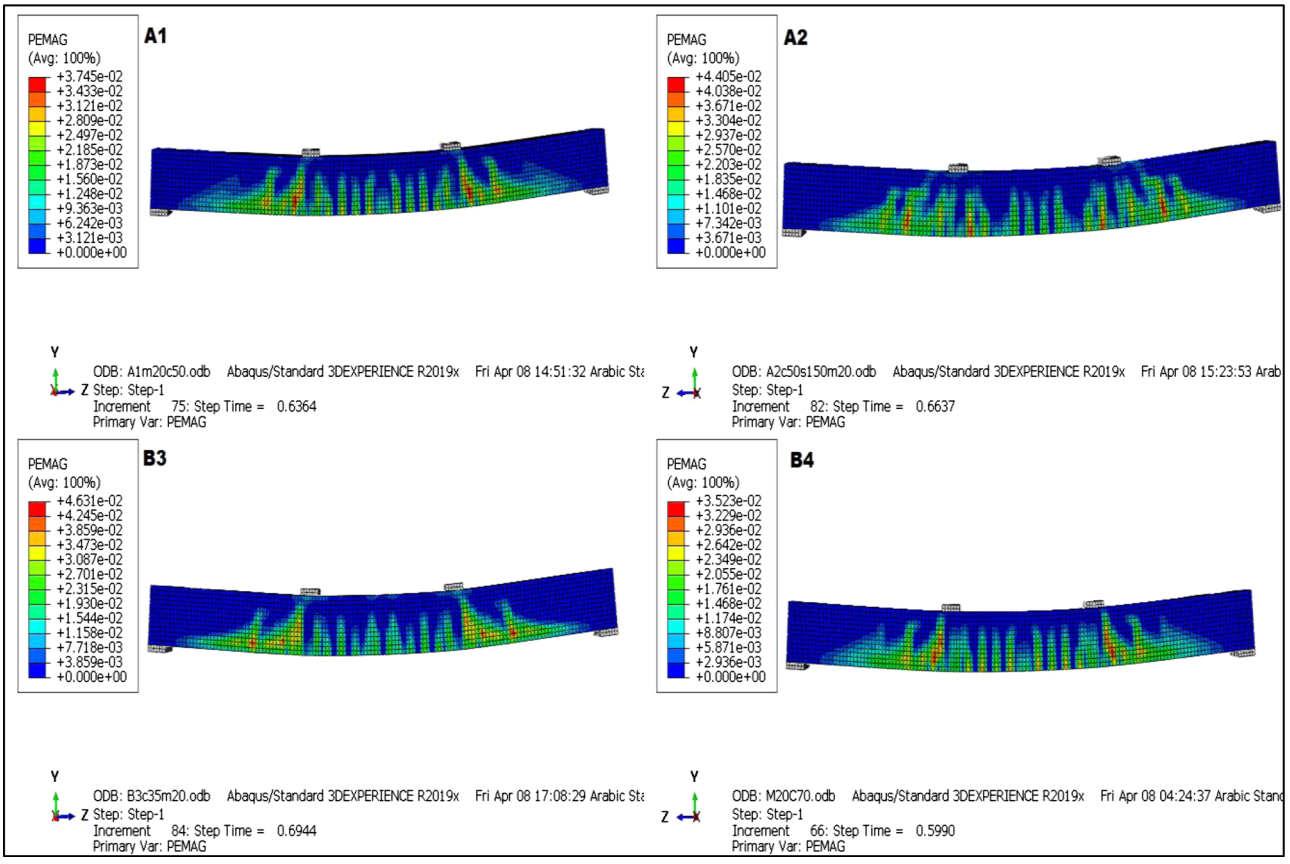

Figure 17: Cracks' pattern.

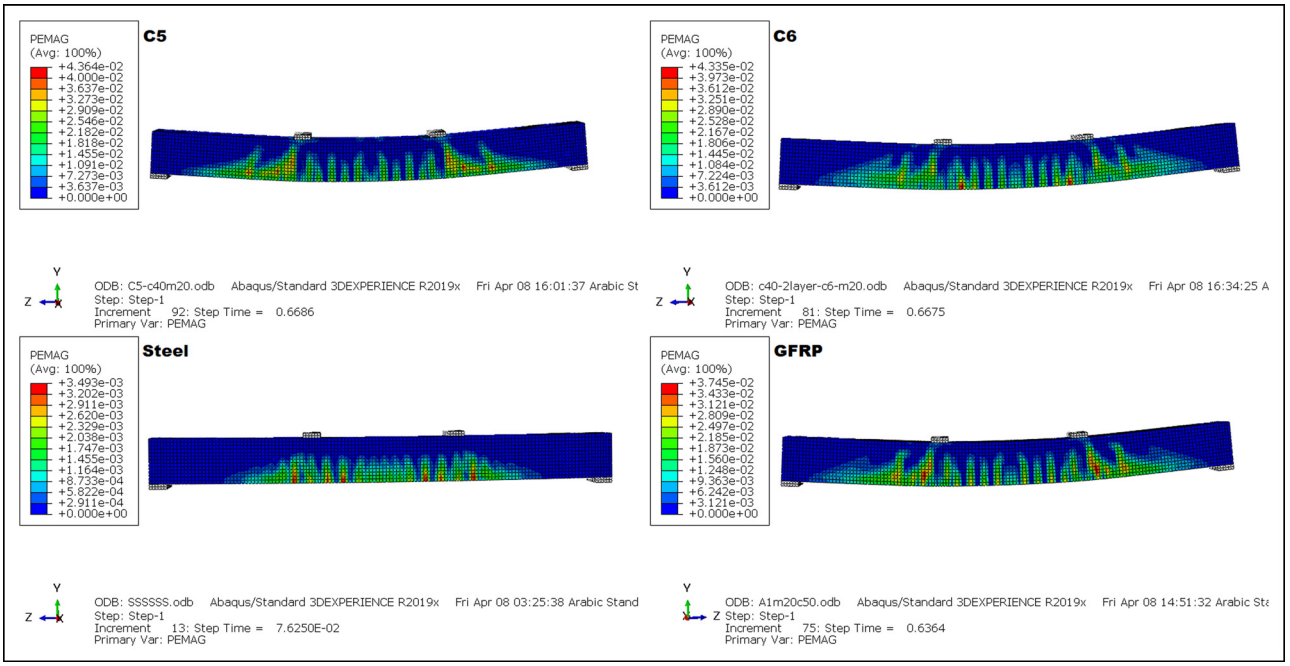

Figure 18: Cracks' pattern.

in the bar, unlike the high ductility of steel. Accordingly, the results of the analysis were as follows:

A. In this group, it is noted that the effect of changing the spacing between stirrups on the load capacity of the beams was not very noticeable. The A1 model failed at a load of 151 kN and the A2 model at 150 kN, though the amount of deflection was slightly less in the A1 model by 2.7% than in the A2 model, with values of 71 and 73 mm, respectively (Figure 6). In terms of strains, the concrete strain in the compression zone of the A1 model approached the ultimate by an amount of 0.0029. Still, this value decreased by 29% in the A2 model to become 0.0023 (Figure 7). As for the strain values in the GFRP bar in the tension region, the strain values were close and with a difference in the A2 model from the A1 by about 3.25%, with values of 0.0016 and 0.00155, respectively (Figure 8).
B. In the second group, the change in the ultimate load capacity was straightforward and relatively more. The effect of changing the compressive strength of concrete from 35 to 70 MPa led to an increase in the final load capacity of the B4 model by 8.4% compared to the B3 model from 143 to 155 kN. The percentage of deflection in the B4 model also decreased by 15.15% compared to the B3 model and by an amount of deflection from 76 to 66 mm, respectively, due to the increase in the compressive strength of concrete (Figure 9). In the strains, the concrete in the compression zone had another opinion, where the difference was somewhat significant due to the doubled increase in the compressive strength of the concrete, where the strain rate decreased in the B4 model by 58% from the B3 model, with strain values 0.005 and 0.0021, respectively (Figure 10). Regarding the GFRP bar in the tensile region, the rate of change in the strain of the two beams was very close, as is the case in the first group, with a difference of 1.9% and with values of 0.0016 and 0.00157, respectively (Figure 11).
C. In the third group, the variables were in the reinforcing layers. The results were different in the load capacity between the two beams, where the load capacity of the C6 model decreased from the C5 model by 17.75% by 146 kN for the C5 model and 124 kN for the C6 model. Still, the amount of deflection was equal at that point for the two beams and was 73 mm (Figure 12). As for the concrete strain in the compression zone, its value decreased in the C6 model by 33.34% from the C5 model with values of 0.0039 and 0.0026, respectively (Figure 13). As for the strain in the bars of the GFRP in the tension zone, it is noted that the strain in the C6 model has increased by a simple 3.6% to the C5 model with values of 0.016 and 0.0166, respectively (Figure 14).

In the fourth group, the modeling and analysis process took place differently from the previous three groups, where a direct comparison was made between a beam reinforced with steel and a beam reinforced with GFRP to understand the general behavior of the GFRP bar against the behavior of steel bar. As expected, the load capacity of the beam reinforced with steel is 30% less than that reinforced with GFRP (105 and 151 kN, respectively). Still, the deflection percentage in the steel model is 83.8% less than the GFRP model (11.5 and 71 mm, respectively), and this difference is due to the low modulus of elasticity that GFRP possesses compared to steel (Figure 15). In terms of strain, both steel and GFRP have reached the ultimate strain. It is noted that the steel strain continues until rupture (Figure 16).

On the other hand, GFRP-reinforced concrete beams had substantially larger cracks before the collapse but were less ductile than steel-reinforced concrete beams, which showed fewer cracks as shown in Figures 17 and 18.

3 Conclusion

- Reducing the spacing between the stirrups from the design spacing approved for the resistance of the shear does not lead to an increase in the ultimate load capacity, but it has the effect of increasing the number of cracks and reducing their width.
- Increasing the compressive strength of concrete leads to an increase in the ultimate load capacity of the beams by up to twice as much from 143 to 155 kN an increase of about 8.4%. In contrast, the percentage of strains decreases in the high compressive strength of concrete.
- Increasing the number of reinforcing layers does not lead to an increase in the ultimate load capacity of the beams and does not affect the percentage of deflection at equal reinforcement values. However, the amount of strain decreases in the beam with two layers of reinforcement in the C6 model by 33.34% from the C5 model.
- The ultimate load capacity of the GFRP beam is higher than that of a beam reinforced with steel, but the amount of deflection is higher in GFRP compared to steel, so the load capacity of the beam reinforced with steel is 30% less than that reinforced with GFRP (105 and 151 kN, respectively). Still, the deflection percentage in the steel model is 83.8% less than the GFRP model (11.5 and 71 mm, respectively).
- The number and width of cracks are more significant in the beam reinforced by GFRP than in the beam reinforced by steel. In general, the serviceability

represented by cracks and deflection is less in the beam reinforced by GFRP than the beam reinforced by steel with higher serviceability. On the other hand, the results showed the expected behavior of GFRP which is linear elastic to the failure stage. In addition, there is no yielding point.

Funding information: The authors state no funding involved.

Author contributions: All authors have accepted responsibility for the entire content of this manuscript and approved its submission.

Conflict of interest: The authors state no conflict of interest.

References

[1] Said AbdulMuttalib I, Abbas OM. Evaluation of deflection in high strength concrete (HSC) I-beam reinforced with carbon fiber reinforced polymer (CFRP) bars. The 7th Asia Pacific Young Researchers and Graduates Symposium. Innovations in Materials and Structural Engineering Practices; 2018. p. 519–33.

[2] Said AbdulMuttalib I, Tu'ma NH. Numerical modeling for flexural behavior of UHPC beams reinforced with steel and sand-coated CFRP bars. IOP Conf Series Earth Environ Sci. 2021;856:012003. doi: 10.1088/1755-1315/856/1/012003.

[3] Said AbdulMuttalib I, Abbas OM. Serviceability behavior of high strength concrete I-beams reinforced with carbon fiber reinforced polymer bars. J Eng. 2013;19(11):1515–30.

[4] Dybel P, Kucharska M, Rzadzka I. Analysis of flexural strength of beam elements reinforced with GFRP bars. IOP Conf Series Mater Sci Eng. 2020;960:032068. doi: 10.1088/1757-899X/960/3/032068.

[5] Ramachandra Murthy A, Pukazhendhi DM, Vishnuvardhan S, Saravanan M, Gandhi P. Performance of concrete beams reinforced with GFRP bars under monotonic loading. Structures. 2020;27:1274–88.

[6] ACI 440.1R-15. Guide for the design and construction of concrete reinforced with FRP bars. Farmington Hills (MI), USA: American Concrete Institute; 2015.

[7] Saraswathy T, Dhanalakshmi K. Investigation of flexural behaviour of RCC beams using GFRP bars. Int J Sci Eng Res. 2014;5(1):333–8.

[8] Besseling JF. A theory of elastic, plastic, and creep deformations of an initially isotropic material showing anisotropic strain-hardening, creep recovery, and secondary creep. J Appl Mech. 1958;25(4):529–36.

[9] Lu Z-H, Zhao Y-G. Empirical stress–strain model for unconfined high-strength concrete under uniaxial compression. J Mater Civ Eng. 2010;22(11):1181–6.

[10] Malm R. Shear cracks in concrete structures subjected to in-plane stresses [dissertation]. Stockholm: Royal Institute of Technology (KTH); 2006.

[11] Genikomsou AS, Polak MA. Finite element analysis of punching shear of concrete slabs using damaged plasticity model in ABAQUS. Eng Struct. 2015;98:38–48.